



Title	TCGA whole-transcriptome sequencing data reveals significantly dysregulated genes and signaling pathways in hepatocellular carcinoma
Author(s)	Ho, DWH; Kai, AKL; Ng, IOL
Citation	Frontiers of Medicine, 2015, v. 9, n. 3, p. 322-330
Issued Date	2015
URL	http://hdl.handle.net/10722/212083
Rights	This work is licensed under a Creative Commons Attribution-NonCommercial-NoDerivatives 4.0 International License.

TCGA whole-transcriptome sequencing data reveals significantly dysregulated genes and signaling pathways in hepatocellular carcinoma

Daniel Wai-Hung Ho, Alan Ka-Lun Kai, Irene Oi-Lin Ng (✉)

Department of Pathology and State Key Laboratory for Liver Research, The University of Hong Kong, Hong Kong SAR, China

© Higher Education Press and Springer-Verlag Berlin Heidelberg 2015

Abstract This study systematically evaluates the TCGA whole-transcriptome sequencing data of hepatocellular carcinoma (HCC) by comparing the global gene expression profiles between tumors and their corresponding non-tumorous liver tissue. Based on the differential gene expression analysis, we identified a number of novel dysregulated genes, in addition to those previously reported. Top-listing upregulated (*CENPF* and *FOXMI*) and downregulated (*CLEC4G*, *CRHBP*, and *CLEC1B*) genes were successfully validated using qPCR on our cohort of 65 pairs of human HCCs. Further examination for the mechanistic overview by subjecting significantly upregulated and downregulated genes to gene set enrichment analysis showed that different cellular pathways were involved. This study provides useful information on the transcriptomic landscape and molecular mechanism of hepatocarcinogenesis for development of new biomarkers and further in-depth characterization.

Keywords TCGA; whole-transcriptome sequencing; HCC; liver cancer

Introduction

Hepatocellular carcinoma (HCC) is a common type of cancer and one of the leading causes of cancer-related mortality worldwide [1,2]. HCC is an aggressive malignancy and patients with HCC have a poor prognosis. Unfortunately, only a few effective treatment options are available. Despite much effort in studying the molecular mechanism of HCC carcinogenesis, current understanding on this lethal disease is still limited.

In the past, delineating the underlying genome-wide HCC regulatory and interaction networks primarily relied on microarray-based technology [3–7]. Recent advancement in next-generation sequencing facilitated the realization of whole-transcriptome sequencing (WTS). This new technological platform allows more comprehensive and accurate examination of global gene expression profile. Currently, only a few studies have utilized WTS strategies in delineating the transcriptomic landscape of HCC [8,9] or liver cancer stem cells [10]. However, all of them are

limited by small sample size in providing a comprehensive and representative overview of HCC transcriptome. The Cancer Genome Atlas (<http://cancergenome.nih.gov/>) represents a global collaboration in cancer research. It has large collections of tissue samples, which were examined in multiple aspects (e.g., genomic, transcriptomic, and epigenetic). More importantly, the data are of open access and freely available to all researchers for use in their own studies. Therefore, the relatively large TCGA HCC WTS data set was utilized in the discovery of the current study.

In our study, we extracted WTS data from the collections of free-access repositories from all 50 HCC cases, in which tumorous (T) and their corresponding non-tumorous (NT) liver tissue was available and analyzed by TCGA. We compared global gene expression profiles between T and NT liver tissue and identified differentially expressed (DE) genes. Top-listing genes were validated by quantitative PCR (qPCR) by using an independent sample cohort ($n = 65$). DE genes were then subjected to gene set enrichment analysis, and we identified gene sets and signaling pathways that were significantly enriched with upregulated and downregulated genes. These genes are attractive molecular targets and are worthy of further investigation, and they may be used as HCC biomarkers.

Received January 14, 2015; accepted May 25, 2015

Correspondence: iolng@hku.hk

1 Materials and methods

TCGA WTS data of HCC

5 From the TCGA data portal (<http://cancergenome.nih.gov/>), we extracted all available WTS data of HCC (a total of 50 cases), which have both T and their corresponding NT samples, through bulk download mode [liver HCC (cancer type), RNASeqV2 (data type), level 3 (archive type) and 1.12.0 (data version)]. The data were generated based on 10 Illumina HiSeq 2000 platform and annotated to reference transcript set of UCSC hg19 gene standard track. Gene expression data were available as upper quartile normalized RSEM count estimates. Extracted data were used 15 without further transformation, except by rounding off values to integers.

Validation sample cohort of paired HCCs

20 A cohort of 65 surgically resected HCCs and their corresponding NT livers were randomly selected for validation. The specimens were collected from patients who underwent surgical resection for HCC at Queen Mary Hospital, Hong Kong. All of them were obtained 25 immediately after surgical resection, snap-frozen in liquid nitrogen and kept at -80°C . Each case had both frozen tissue blocks and formalin-fixed paraffin-embedded tissue; frozen sections were cut from tumor blocks and stained for histological examination to ensure a homogenous cell 30 population of tissue. The use of the tissue was approved by the Institutional Review Board of the University of Hong Kong/Hospital Authority Hong Kong West Cluster. The demographic data of the patients are summarized in Supplementary Table 1.

35 Differential gene expression detection

Differential gene expression (DGE) analysis was performed using edgeR [11]. It uses negative binomial models 40 to capture variance dispersion for WTS read count data, empirical Bayes estimation for gene-specific variation, and generalized linear models applicable to general experiments. As suggested by edgeR, genes with very low read counts are usually not of interest in DGE analysis; hence, 45 average count-per-million (CPM) was used to determine whether a gene was reasonably expressed or not. Subsequently, \log_2 (fold change), \log_2 (CPM), statistical significance, and the corresponding false discovery rate (FDR) were reported by edgeR. DE genes were selected 50 based on these parameters, with the T/NT expression fold change (FC) denoting upregulation or downregulation.

Gene set enrichment analysis on DE genes

55 To evaluate the mechanistic overview of DGE for HCC,

the significantly upregulated and downregulated genes were tested for gene set or pathway enrichment by uGPA package [12]. Enrichment analyses of the upregulated and downregulated genes were performed separately as recommended previously [13]. Curated gene sets were 5 obtained from MSigDB v4.0 (www.broadinstitute.org/gsea/msigdb) and classified into functional gene sets according to the domains of gene ontology (GO) [i.e., biological process (825 gene sets), cellular component (233 gene sets), and molecular function (396 gene sets)] or 10 pathway gene sets according to canonical pathways as documented by KEGG (186 gene sets). uGPA takes DGE events as input and assesses them for enrichment events within gene sets or signaling pathways by cumulative hypergeometric test. An FDR of < 0.05 was treated as 15 significant event.

Validation on top-listing gene candidates by qPCR in human HCCs

To confirm the WTS findings on DGE, the top-listing upregulated (*CENPF* and *FOXMI*) and downregulated (*CLEC4G*, *CRHBP*, and *CLEC1B*) genes were subjected to qPCR by TaqMan real-time qPCR assays 25 (Hs01118845_m1, Hs01073586_m1, Hs00962163_g1, Hs00181810_m1, and Hs00212925_m1), following manufacturer's instructions. Total RNA was extracted by Trizol (Invitrogen) and cDNA was synthesized by reverse transcription kit (Life Technologies) on the validation sample cohort ($n = 65$). 30

Results

Comparison of global gene expression profiles of HCC T and NT tissue

By comparing the WTS read counts of the various genes between T and NT tissue and subsequently applying the selection criteria of $\log_2(\text{FC}) \geq 2$, $\log_2(\text{CPM}) \geq 1$, and $\text{FDR} < 0.05$, 734 genes were regarded as having DGE, 40 among which 220 were upregulated and 514 were downregulated (Fig. 1). In terms of statistical significance, *CENPF* (centromere protein F, 350/400 kDa) ($\log_2\text{FC} = 3.64$, $\text{FDR} = 5.32\text{E-}78$) and *CLEC4G* (C-type lectin domain family 4, member G) ($\log_2\text{FC} = -8.96$, $\text{FDR} = 1.19\text{E-}80$) were the most significantly upregulated and 45 downregulated genes, respectively (Supplementary Tables 2 and 3).

Successful validation of top-listing candidates by qPCR

Top-listing upregulated (*CENPF* and *FOXMI*) and downregulated (*CLEC4G*, *CRHBP*, and *CLEC1B*) genes were subjected to qPCR assays on our validation sample cohort of 65 HCC pairs. All of these genes were found to be 55

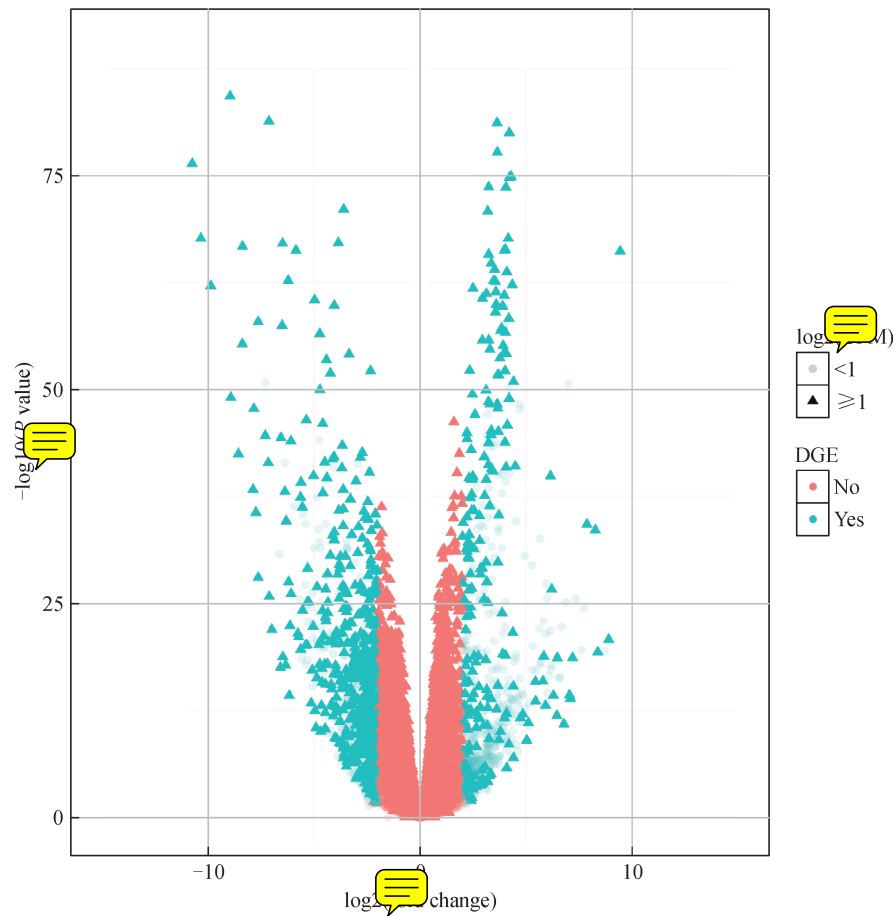


Fig. 1 Volcano plot of the WTS data. The color of the data points denotes the status of DGE and the intensity (light vs. dark) and shape (round dot vs. triangle) of the data points denote the average expression level of genes as defined by $\log_2(\text{CPM})$ (< 1 vs. ≥ 1).

successfully validated ($P < 0.0001$, Mann-Whitney U test) and the dysregulation trend matched with those observed in the TCGA WTS data (Fig. 2).

Significantly enriched pathways for upregulated and downregulated genes

By subjecting the significantly upregulated genes to enrichment analysis on gene sets based on GO (i.e., biological process, cellular component, and molecular function) and KEGG canonical pathways, we observed that upregulated genes were significantly enriched in various domains (Table 1). For GO biological process, the genes were mainly enriched in cell cycle processes. For GO cellular component, non-membrane-bound organelles and cytoskeleton were involved. For GO molecular function, motor activity and various binding activities were implicated. Based on the canonical signaling pathways documented in KEGG, pathways on cell cycle and p53 signaling were significantly enriched.

Meanwhile, downregulated genes were also subjected to gene set enrichment analysis (Table 2). For GO biological process, the genes were mainly related to signal transduction, response to stimulus, and various metabolic processes. For GO cellular component, they were implicated in membrane and extracellular matrix (ECM). For GO molecular function, they were involved in versatile types of activities including oxygen binding, receptor activity, and oxidoreductase activity. They were also enriched in canonical signaling pathways that are related to metabolism of various substrates.

Discussion

In the current study, we made use of the T-NT TCGA WTS data extracted from 50 HCC pairs to provide useful transcriptomic landscape for HCC. We systematically compared the gene expression profiles of HCC T samples with their corresponding NT samples, and identified 734

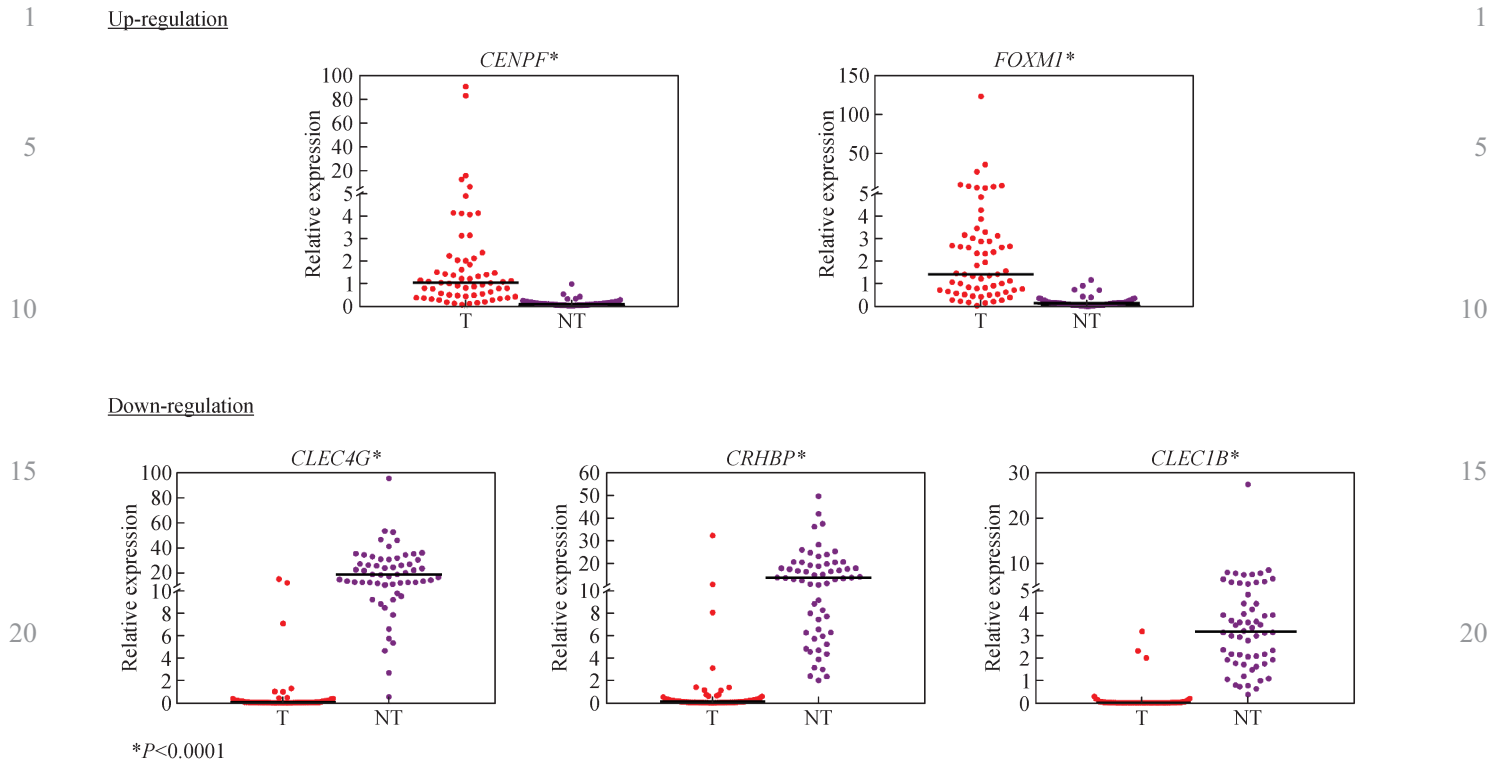


Fig. 2 Successful qPCR validation of top-listing DE genes.

Table 1 Summary of gene set enrichment analysis on significantly upregulated genes

Gene set	# of genes	# of DE genes	P value	FDR	DE genes
GO biological process					
MITOTIC_CELL_CYCLE	153	27	6.91E-33	5.70E-30	<i>PRC1, PKMYT1, AURKA, CDKN2A, CDKN2C, CCNA2, CDCA5, MAD2L1, ZWINT, NEK2, ANLN, NDC80, PLK1, E2F1, KIF23, KIF2C, DLGAP5, CDC6, KIF11, UBE2C, BUB1B, NCAPH, BUB1, CENPF, BIRC5, CENPE, CDKN3</i>
CELL_CYCLE_PROCESS	193	28	1.48E-31	6.09E-29	<i>AURKA, CDCA5, CCNA2, MAD2L1, ZWINT, NEK2, NDC80, CDC6, NCAPH, BUB1, BIRC5, CDKN3, PRC1, PKMYT1, CDKN2A, CDKN2C, ANLN, PLK1, E2F1, KIF23, KIF2C, DLGAP5, KIF11, UBE2C, BUB1B, CENPF, CENPE, RACGAP1</i>
CELL_CYCLE_GO_0007049	315	32	6.90E-31	1.90E-28	<i>AURKA, CCNA2, CDCA5, MAD2L1, ZWINT, NEK2, NDC80, CDC20, CDT1, CDC6, NCAPH, CDC45, BUB1, BIRC5, CDKN3, PRC1, PKMYT1, CDKN2A, CDKN2C, ANLN, PLK1, E2F1, KIF23, KIF2C, DLGAP5, KIF11, MCM2, UBE2C, BUB1B, CENPF, CENPE, RACGAP1</i>
CELL_CYCLE_PHASE	170	25	2.02E-28	4.17E-26	<i>PKMYT1, AURKA, CDKN2A, CDKN2C, CDCA5, CCNA2, MAD2L1, ZWINT, NEK2, ANLN, NDC80, PLK1, E2F1, KIF2C, DLGAP5, CDC6, KIF11, UBE2C, BUB1B, NCAPH, BUB1, CENPF, BIRC5, CENPE, CDKN3</i>
M_PHASE_OF_MITOTIC_CELL_CYCLE	85	19	1.49E-25	2.45E-23	<i>PKMYT1, AURKA, KIF2C, DLGAP5, CDCA5, CCNA2, KIF11, UBE2C, MAD2L1, ZWINT, BUB1B, NEK2, ANLN, NCAPH, BUB1, BIRC5, NDC80, CENPE, PLK1</i>

(Continued)

Gene set	# of genes	# of DE genes	<i>P</i> value	FDR	DE genes
GO cellular component					
NON_MEMBRANE_BOUND_ORGANELLE	631	29	2.11E-18	2.46E-16	<i>CDCA5, ZWINT, KIF4A, NDC80, MAPT, CDK1, BUB1, CCNB2, PRC1, CDKN2A, ACTN2, ANLN, PLK1, KIF23, KIF2C, DLGAP5, KIF11, NEB, AURKA, MAD2L1, NEK2, CDC20, CDT1, TOP2A, BIRC5, MCM2, BUB1B, CENPF, CENPE</i>
INTRACELLULAR_NON_MEMBRANE_BOUND_ORGANELLE	631	29	2.11E-18	2.46E-16	<i>CDCA5, ZWINT, KIF4A, NDC80, MAPT, CDK1, BUB1, CCNB2, PRC1, CDKN2A, ACTN2, ANLN, PLK1, KIF23, KIF2C, DLGAP5, KIF11, NEB, AURKA, MAD2L1, NEK2, CDC20, CDT1, TOP2A, BIRC5, MCM2, BUB1B, CENPF, CENPE</i>
MICROTUBULE_CYTOSKELETON	152	17	1.36E-17	1.05E-15	<i>PRC1, AURKA, KIF4A, NEK2, CDC20, PLK1, KIF23, KIF2C, DLGAP5, MAPT, TOP2A, KIF11, CDK1, BUB1, CENPF, BIRC5, CCNB2</i>
SPINDLE	39	11	1.51E-16	8.81E-15	<i>KIF23, KIF4A, PRC1, AURKA, DLGAP5, BUB1, KIF11, CDK1, CENPF, BIRC5, CDC20</i>
CYTOSKELETAL_PART	235	18	1.29E-15	6.03E-14	<i>AURKA, KIF4A, NEK2, CDC20, MAPT, TOP2A, CDK1, BUB1, BIRC5, PRC1, ACTN2, ANLN, PLK1, KIF23, KIF2C, DLGAP5, KIF11, CENPF</i>
GO molecular function					
MICROTUBULE_MOTOR_ACTIVITY	16	5	1.96E-08	7.77E-06	<i>KIF23, KIF4A, KIF11, CENPE, KIF2C</i>
MOTOR_ACTIVITY	28	5	4.19E-07	8.29E-05	<i>KIF23, KIF4A, KIF2C, KIF11, CENPE</i>
CYTOSKELETAL_PROTEIN_BINDING	159	7	2.97E-05	0.004	<i>NRCAM, ACTN2, ANLN, MAPT, BIRC5, RACGAP1, MAPK8IP2</i>
CARBOHYDRATE_BINDING	72	5	4.90E-05	0.005	<i>REG3A, CD34, MDK, THBS4, LPL</i>
PROTEIN_KINASE_REGULATOR_ACTIVITY	39	4	6.21E-05	0.005	<i>SFN, CDKN2A, CDKN2C, MAPK8IP2</i>
KEGG pathway					
KEGG_CELL_CYCLE	128	19	6.25E-22	1.16E-19	<i>CDC45, PLK1, CCNA2, BUB1, MCM2, PTTG1, CDC6, CDC20, CCNB1, CCNE1, SFN, E2F1, CDK1, BUB1B, MAD2L1, CDKN2A, CDKN2C, PKMYT1, CCNB2</i>
KEGG_OOCYTE_MEIOSIS	114	11	4.06E-11	3.78E-09	<i>PLK1, BUB1, PTTG1, CDC20, CCNB1, CCNE1, CDK1, MAD2L1, AURKA, PKMYT1, CCNB2</i>
KEGG_PROGESTERONE_MEDIATED_OOCYTE_MATURATION	86	8	2.62E-08	1.63E-06	<i>CDK1, MAD2L1, PLK1, CCNA2, BUB1, PKMYT1, CCNB2, CCNB1</i>
KEGG_P53_SIGNALING_PATHWAY	69	7	1.09E-07	5.06E-06	<i>SFN, CDK1, CDKN2A, RRM2, CCNB2, CCNB1, CCNE1</i>
KEGG_TIGHT_JUNCTION	134	4	0.006	0.226	<i>MYH4, ACTN2, CTNNA2, PPP2R2C</i>

Table 2 Summary of gene set enrichment analysis on significantly downregulated genes

Gene set	# of genes	# of DE genes	<i>P</i> value	FDR	DE genes
GO biological process					
SIGNAL_TRANSDUCTION	1634	70	9.98E-19	8.24E-16	<i>DIRAS3, IGF1, IGF2, HPGD, GNA14, MARCO, CCL3, ADRA2B, TBXA2R, ADRA1B, ADRA1A, WNK2, IL1RL1, NR1I2, CXCL6, GRIA3, FCGR2B, GABRB3, CAMK2B, BCL2L10, AVPR1A, TRPV4, CCL19, NPY1R, APOA1, NR4A3, ESR1, CHRNA4, LILRB5, PDGFRA, ECM1, TNFRSF11B, GADD45G, GADD45B, CLEC1B, IL18R1, SOCS2, SOCS3, PTH1R, CTNND2, PTPRD, CRHBP, LIFR, CEACAM6, FPR1, CXCL12, NR4A1, CXCL14, SKAP1, WISP2, MCC, RND2, TACSTD2, EPHA2, NTRK2, TGFA, CHL1, LY6E, VIPR1, CD79A, IGFBP1, PRKAR2B, RET, RCAN1, ANXA3, SFRP5, SFRP1, GCGR, IGFALS, DTX1</i>

						(Continued)	
Gene set	# of genes	# of DE genes	<i>P</i> value	FDR	DE genes		
1	RESPONSE_TO_EXTERNAL_STIMULUS	312	25	5.02E-13	2.07E-10	<i>SLI00A8, SERPINE1, F9, SAA1, IL1RAP, TRPV4, CXCL2, FPR1, CXCL6, GCGR, CCL21, LECT2, CCL19, CD1D, ORM1, SELE, CXCL12, PGLYRP2, CCL3, ALB, LYVE1, CXCL14, CXCL13, FOS, MBL2</i>	1
5	CARBOXYLIC_ACID_METABOLIC_PROCESS	178	19	2.13E-12	5.38E-10	<i>SLC7A8, BBOX1, ASPA, GGT5, CYP39A1, ACOT12, GSTZ1, SLC3A1, SDS, HAO2, AKR1D1, SLC27A5, GLS2, FTCD, IGF1, CYP4A11, GLYAT, GCK, HPGD</i>	5
	ORGANIC_ACID_METABOLIC_PROCESS	180	19	2.61E-12	5.38E-10	<i>SLC7A8, BBOX1, ASPA, GGT5, CYP39A1, ACOT12, GSTZ1, SLC3A1, SDS, HAO2, AKR1D1, SLC27A5, GLS2, FTCD, IGF1, CYP4A11, GLYAT, GCK, HPGD</i>	10
10	LIPID_METABOLIC_PROCESS	325	24	8.36E-12	1.38E-09	<i>CYP3A4, ALDH8A1, LCAT, APOF, PITPNM3, NR1I2, CYP39A1, CETP, THRSP, HAO2, SLC27A5, HPGD, APOA4, APOA1, BCO2, ACOT12, NPC1L1, IP6K3, AKR1D1, CYP4A11, GLYAT, RDH16, UGT2B7, SMPD3</i>	10
15	GO cellular component MEMBRANE	1994	90	1.23E-25	2.87E-23	<i>IL1RAP, GHR, SLC22A1, CFTR, SLC3A1, C8A, GNA14, MARCO, ADRA2B, LYVE1, TBXA2R, ADRA1B, ADRA1A, TREH, CA9, CD4, GPR128, ABCB11, STEAP4, CD163, GRIA3, CD1D, SLC16A4, GABRB3, NAPS, CNGA1, PLEKHB1, PTPRS, AVPRIA, UNC93A, TRPV4, SELP, NPY1R, SELE, SLC34A2, NCAM1, CNTFR, MRC1, HS3ST3A1, MAN1C1, SLCO1B3, CHRNA4, CLEC4M, PDGFRA, HS3ST3B1, CLEC1B, IL18R1, PKHD1, PTH1R, RHBG, CRI, PTPRD, LIFR, SRPX, CEACAM6, C7, C9, FPR1, STAB2, SLC13A2, CLDN2, PRSS8, GGT5, EPCAM, TACSTD2, MME, EPHA2, NTRK2, CHL1, LY6E, PROM1, VIPRI, FXYD1, ITGB8, ITGA9, CD79A, SLC5A1, NGFR, PITPNM3, CDHR2, SLC7A8, KCND3, B3GAT1, SIGLEC7, VSIG2, CLDN10, GCGR, SLC6A2, BASP1, SLC10A1</i>	15
20							20
25	PLASMA_MEMBRANE	1426	75	2.65E-25	3.09E-23	<i>LIFR, IL1RAP, CEACAM6, SLC22A1, GHR, CFTR, SLC3A1, C9, FPR1, STAB2, GNA14, MARCO, ADRA2B, LYVE1, ADRA1B, TBXA2R, SLC13A2, ADRA1A, TREH, CLDN2, PRSS8, CD4, ABCB11, EPCAM, TACSTD2, MME, EPHA2, NTRK2, STEAP4, CD163, LY6E, GRIA3, CD1D, PROM1, SLC16A4, GABRB3, VIPRI, CNGA1, FXYD1, ITGB8, ITGA9, CD79A, SLC5A1, NGFR, PTPRS, AVPRIA, UNC93A, TRPV4, SELP, NPY1R, SELE, SLC7A8, KCND3, SLC34A2, NCAM1, MRC1, SIGLEC7, SLCO1B3, CHRNA4, CLEC4M, VSIG2, PDGFRA, HS3ST3B1, CLEC1B, CLDN10, GCGR, IL18R1, SLC6A2, BASP1, PKHD1, PTH1R, RHBG, CRI, PTPRD, SLC10A1</i>	25
30							30
35	INTRINSIC_TO_MEMBRANE	1348	72	1.09E-24	8.46E-23	<i>LIFR, IL1RAP, CEACAM6, SLC22A1, GHR, SLC3A1, C8A, C7, C9, FPR1, STAB2, MARCO, ADRA2B, LYVE1, TBXA2R, ADRA1B, ADRA1A, SLC13A2, TREH, CA9, GPR128, ABCB11, GGT5, TACSTD2, MME, EPHA2, NTRK2, CD163, CHL1, LY6E, CD1D, PROM1, SLC16A4, GABRB3, VIPRI, CNGA1, FXYD1, ITGB8, ITGA9, SLC5A1, PLEKHB1, NGFR, PTPRS, PITPNM3, CDHR2, AVPRIA, SELP, NPY1R, SLC7A8, KCND3, SLC34A2, NCAM1, MRC1, B3GAT1, SIGLEC7, HS3ST3A1, MAN1C1, SLCO1B3, CHRNA4, CLEC4M, VSIG2, PDGFRA, HS3ST3B1, CLEC1B, GCGR, SLC6A2, PKHD1, PTH1R, RHBG, CRI, PTPRD, SLC10A1</i>	35
40							40
45	INTEGRAL_TO_MEMBRANE	1330	70	1.21E-23	7.03E-22	<i>LIFR, IL1RAP, CEACAM6, GHR, SLC22A1, SLC3A1, C8A, C7, C9, FPR1, STAB2, MARCO, ADRA2B, LYVE1, ADRA1B, TBXA2R, ADRA1A, SLC13A2, CA9, GPR128, ABCB11, GGT5, TACSTD2, MME, EPHA2, NTRK2, CD163, CHL1, LY6E, CD1D, PROM1, SLC16A4, GABRB3, VIPRI, CNGA1, FXYD1, ITGB8, ITGA9, SLC5A1, PLEKHB1, NGFR, PTPRS, PITPNM3, CDHR2, AVPRIA, SELP, NPY1R, SLC7A8, KCND3, SLC34A2, NCAM1, MRC1, B3GAT1, SIGLEC7, HS3ST3A1, MAN1C1, SLCO1B3, CHRNA4, CLEC4M, VSIG2, PDGFRA, HS3ST3B1, CLEC1B, GCGR, SLC6A2, PKHD1, PTH1R, RHBG, CRI, PTPRD, SLC10A1</i>	45
50							50
55							55

(Continued)

Gene set	# of genes	# of DE genes	<i>P</i> value	FDR	DE genes
MEMBRANE_PART	1670	78	4.27E-23	1.99E-21	<i>IL1RAP, SLC22A1, GHR, CFTR, SLC3A1, C8A, GNA14, MARCO, ADRA2B, LYVE1, TBXA2R, ADRA1B, ADRA1A, TREH, CA9, GPR128, ABCB11, CD163, CD1D, SLC16A4, GABRB3, CNGA1, PLEKHB1, PTPRS, AVPRIA, SELP, NPY1R, SLC34A2, NCAMI, CNTFR, MRC1, HS3ST3A1, MAN1C1, SLCO1B3, CHRNA4, CLEC4M, PDGFRA, HS3ST3B1, CLEC1B, PKHD1, PTH1R, RHBG, CR1, PTPRD, LIFR, CEACAM6, C7, C9, FPR1, STAB2, SLC13A2, CLDN2, GGT5, TACSTD2, MME, EPHA2, NTRK2, CHL1, LY6E, PROM1, VIPRI, FXYD1, ITGB8, ITGA9, CD79A, SLC5A1, NGFR, PITPNM3, CDHR2, SLC7A8, KCND3, B3GAT1, SIGLEC7, VSIG2, CLDN10, GCGR, SLC6A2, SLC10A1</i>
GO molecular function					
OXYGEN_BINDING	22	12	9.98E-18	3.95E-15	<i>CYP3A4, CYP3A7, CYP1A1, CYP2C19, CYP26A1, CYP1A2, CYP2E1, ALB, CYP2A6, CYP2A7, CYP8B1, HBB</i>
RECEPTOR_ACTIVITY	583	34	3.28E-13	6.50E-11	<i>LIFR, PTPRS, AVPRIA, IL13RA2, GHR, FPR1, STAB2, HPGD, MARCO, PGLYRP2, RET, CNTFR, ADRA2B, GABRP, MRC1, NR4A3, ADRA1B, TBXA2R, ADRA1A, SIGLEC7, MCC, CD4, GPR128, CHRNA4, LILRB5, TACSTD2, PDGFRA, TNFRSF11B, CLEC1B, GCGR, GABRB3, VIPRI, PTH1R, PTPRD</i>
OXIDOREDUCTASE_ACTIVITY	289	24	6.83E-13	9.02E-11	<i>CYP3A4, ALDH8A1, BBOX1, CYP26A1, CYP1A2, GPD1, CYP8B1, CYP39A1, GSTZ1, HAO2, PHGDH, HPGD, ADH1B, AKR7A3, KMO, BCO2, TDO2, SRD5A2, ACADL, CYP2A6, ADH6, ADH4, CYP4A11, RDH16</i>
TRANSMEMBRANE_RECEPTOR_ACTIVITY	418	25	2.78E-10	2.75E-08	<i>LIFR, PTPRS, AVPRIA, IL13RA2, GHR, FPR1, STAB2, HPGD, CNTFR, ADRA2B, GABRP, ADRA1B, TBXA2R, ADRA1A, CD4, GPR128, CHRNA4, LILRB5, PDGFRA, CLEC1B, GCGR, GABRB3, VIPRI, PTH1R, PTPRD</i>
RECEPTOR_BINDING	377	23	9.87E-10	7.82E-08	<i>APOF, PITPNM3, IL1RN, TNFRSF11B, SAA1, TGFA, CXCL2, CXCL6, CCL21, CCL19, IGF1, IGF2, CXCL12, APOA1, SOCS2, CCL3, ANGPTL1, CXCL14, CXCL13, MBL2, ADAMTS13, TNXB, DTX1</i>
KEGG pathway					
KEGG_RETINOL_METABOLISM	64	25	6.92E-31	1.29E-28	<i>CYP4A11, CYP3A4, ADH1B, ADH1C, ADH4, ADH1A, CYP26A1, CYP2C9, CYP2C19, CYP2C8, CYP2B6, CYP2A13, UGT1A4, CYP3A7, LRAT, CYP2A6, CYP2A7, CYP4A22, CYP1A1, CYP1A2, ADH6, UGT2A1, CYP3A43, RDH16, UGT2B7</i>
KEGG_DRUG_METABOLISM_CYTOCHROME_P450	72	23	4.00E-26	3.72E-24	<i>CYP2E1, CYP3A4, GSTZ1, ADH1B, ADH1C, ADH4, ADH1A, CYP2C9, CYP2C19, CYP2C8, CYP2B6, CYP2A13, UGT1A4, CYP3A7, GSTM5, GSTA2, CYP2A6, CYP2A7, CYP1A2, ADH6, UGT2A1, CYP3A43, UGT2B7</i>
KEGG_METABOLISM_OF_XENOBIOTICS_BY_CYTOCHROME_P450	70	21	2.63E-23	1.63E-21	<i>CYP2E1, CYP3A4, GSTZ1, ADH1B, ADH1C, ADH4, ADH1A, CYP2C9, CYP2C19, CYP2C8, CYP2B6, UGT1A4, CYP3A7, GSTM5, GSTA2, CYP1A1, CYP1A2, ADH6, UGT2A1, CYP3A43, UGT2B7</i>
KEGG_DRUG_METABOLISM_OTHER_ENZYMES	51	12	1.75E-12	8.13E-11	<i>CYP3A4, UPP2, CDA, CYP2A13, UGT1A4, CYP3A7, CYP2A6, CYP2A7, UGT2A1, CYP3A43, NAT2, UGT2B7</i>
KEGG_LINOLEIC_ACID_METABOLISM	29	9	6.96E-11	2.59E-09	<i>CYP2E1, CYP3A4, CYP1A2, PLA2G2A, CYP3A43, CYP2C9, CYP2C19, CYP2C8, CYP3A7</i>

DE genes. A number of DE genes that were reported in previous studies [8,9], such as *ALGIL*, *SERPINA11*, *TMEM82*, *GPC3*, *SPINK1*, and *ESM1*, were also detected in the current study. In addition, many other novel genes were found to be significantly upregulated (Supplementary

Table 2) and downregulated (Supplementary Table 3). *CENPF* (centromere protein F) and *FOXMI* (forkhead box M1) were among the top-listing significantly upregulated genes. *CENPF* is required for kinetochore function and chromosome segregation in mitosis. On the other hand,

1 FOXM1 is a transcription factor that regulates the
 expression of cell cycle genes for DNA replication and
 mitosis. It may also have roles in controlling cell
 proliferation and DNA-break repair of DNA damage
 5 checkpoint response. Intriguingly, through an integrative
 computational approach in which the interactomes of
 human and mice were compared, *CENPF* and *FOXM1*
 were predicted to be the master regulators for prostate
 cancer malignancy [14]. Moreover, they were also shown
 10 to act synergistically in driving aggressive prostate cancer.
 Knockdown of *CENPF* and *FOXM1* synergistically
 reduced the proliferation of prostate cancer cells and
 tumor growth in cell-line-derived xenografts. It was further
 shown that knockdown of *CENPF* expression reduced the
 15 binding of FOXM1 to its targets. These two proteins were
 also demonstrated to co-localize in nucleus and their co-
 expression was a robust prognostic indicator of poor
 survival and metastasis. Thus, the concurrent upregulation
 of them in HCC likely suggests a similar synergistic co-
 20 operation in hepatocarcinogenesis.

Among the most significantly downregulated genes, we
 noted multiple members of the C-type lectin family
 (*CLEC4G*, *CLEC1B*, and *CLEC4M*) and *CRHBP* [cortico-
 tropin-releasing factor (CRF) binding protein]. C-type
 25 lectins are calcium-dependent glycan binding proteins and
 function as adhesion and signaling receptors in various
 immune functions, including inflammation and immunity
 to tumor and virally infected cells [15]. According to the
 Human Protein Atlas [16], *CLEC4G*, *CLEC1B*, and
 30 *CLEC4M* are predominantly expressed in liver; however,
CLEC4G and *CLEC4M* are expressed at very low levels or
 are undetectable in liver cancer tissue (data not available
 for *CLEC1B* on liver cancer tissue). This finding suggests
 that disruption of expression of these C-type lectin proteins
 35 may have a role in the pathogenesis of HCC. *CRHBP* is a
 member of the CRF system. Activation of CRF receptors,
 particularly *CRFR2* was shown to inhibit tumor progres-
 sion, modulate proliferation and apoptosis, and interfere
 with angiogenesis through reduction of VEGF expression
 40 *in vivo* in various cancers [17–20]. A recent study also
 indicated that reduced expression of *CRHBP* was asso-
 ciated with a more aggressive behavior of human kidney
 cancer, suggesting depletion of *CRHBP* may be involved
 in renal carcinogenesis [21].


45 Gene set enrichment analysis further provides a
 mechanistic overview of HCC. First, proteins of various
 cell cycle processes were frequently upregulated, particu-
 larly for multiple cyclins and cyclin-dependent kinases
 (*CCNA2*, *CCNB1*, *CCNB2*, *CCNE1*, *CDK1*, *CDKN2A*,
 50 *CDKN2C*, and *CDKN3*) (Supplementary Tables 2 and 4).
 Given that cell cycle is controlled at various checkpoints
 by regulating cyclins, cyclin-dependent kinases and other
 cell cycle proteins [22,23], upregulation of these genes
 may lead to disruption in cell cycle control and result in

1 abnormal cell proliferation. Second, the expression of
 many genes for various metabolic processes was prefer-
 entially downregulated in HCC, including metabolism of
 retinol, fatty acids, amino acids and carbohydrates, steroid
 5 hormone biosynthesis, and glycolysis and gluconeogen-
 esis. In particular, multiple components of cytochrome
 P450 were significantly downregulated in HCC (Supple-
 mentary Tables 3 and 5) and they play critical roles in
 biosynthesis and metabolism [24]. Besides, they are also
 involved in the removal of toxic substances from the body
 10 [25,26]. Meanwhile, numerous cytokines (*CCLs* and
CXCLs) were also downregulated in HCC (Supplementary
 Tables 3 and 5). Cytokines and its receptors are important
 for triggering immune responses through the action of
 various immune cells [27]. These immune responses are
 15 critical in responses against infection [28] and cancer [29].
 Overall, these findings suggest altered metabolic and
 immune systems of HCC compared with non-tumorous
 hepatocytes.

In the initial global analyses of the TCGA WTS data of
 HCC and subsequent validation by an independent sample
 cohort, we discovered several promising gene candidates
 and pathways that are significantly dysregulated in HCC.
 These findings shed light on some novel targets that may
 25 potentially drive hepatocarcinogenesis. However, further
 functional characterization and *in vivo* validation using
 animal model are needed to substantiate our findings.

In conclusion, this study explored the molecular
 mechanism of hepatocarcinogenesis through assessment
 of TCGA WTS data of HCC and validation of some of the
 top-listing DE genes in an independent cohort. It provides
 useful information on the transcriptomic landscape as well
 as a mechanistic overview of HCC. Our findings offer
 30 novel insights and useful support in biomarker develop-
 ment and suggest new potential targets in HCC character-
 ization.

Acknowledgements

The study  supported in part by the SK Yee Medical Research
 Fund 2011 and the Small Project Funding (201309176065). IOL Ng
 is Loke Yew Professor in Pathology.

Compliance with ethics guidelines

Daniel WH Ho, Alan KL Kai, and Irene OL Ng declare that they
 have no conflict of interest. The use of human tissue in this study was
 approved by the Institutional Review Board of the University of
 Hong Kong/Hospital Authority Hong Kong West Cluster (UW 09-
 185).

Electronic Supplementary Material Supplementary material
 is available in the online version of this article at <http://dx.doi.org/10.1007/s11684-015-0408-9> and is accessible for authorized users.

References

1. El-Serag HB. Hepatocellular carcinoma. *N Engl J Med* 2011; 365 (12): 1118–1127
2. Villanueva A, Llovet JM. Liver cancer in 2013: Mutational landscape of HCC—the end of the beginning. *Nat Rev Clin Oncol* 2014; 11(2): 73–74
3. Jia HL, Ye QH, Qin LX, Budhu A, Forgues M, Chen Y, Liu YK, Sun HC, Wang L, Lu HZ, Shen F, Tang ZY, Wang XW. Gene expression profiling reveals potential biomarkers of human hepatocellular carcinoma. *Clin Cancer Res* 2007; 13(4): 1133–1139
4. Lee JS, Thorgeirsson SS. Comparative and integrative functional genomics of HCC. *Oncogene* 2006; 25(27): 3801–3809
5. Marshall A, Lukk M, Kutter C, Davies S, Alexander G, Odom DT. Global gene expression profiling reveals SPINK1 as a potential hepatocellular carcinoma marker. *PLoS ONE* 2013; 8(3): e59459
6. Patil MA, Chua MS, Pan KH, Lin R, Lih CJ, Cheung ST, Ho C, Li R, Fan ST, Cohen SN, Chen X, So S. An integrated data analysis approach to characterize genes highly expressed in hepatocellular carcinoma. *Oncogene* 2005; 24(23): 3737–3747
7. Skawran B, Steinemann D, Weigmann A, Flemming P, Becker T, Flik J, Kreipe H, Schlegelberger B, Wilkens L. Gene expression profiling in hepatocellular carcinoma: upregulation of genes in amplified chromosome regions. *Mod Pathol* 2008; 21(5): 505–516
8. Huang Q, Lin B, Liu H, Ma X, Mo F, Yu W, Li L, Li H, Tian T, Wu D, Shen F, Xing J, Chen ZN. RNA-Seq analyses generate comprehensive transcriptomic landscape and reveal complex transcript patterns in hepatocellular carcinoma. *PLoS ONE* 2011; 6(10): e26168
9. Lin KT, Shann YJ, Chau GY, Hsu CN, Huang CY. Identification of latent biomarkers in hepatocellular carcinoma by ultra-deep whole-transcriptome sequencing. *Oncogene* 2014; 33(39): 4786–4794
10. Ho DW, Yang ZF, Yi K, Lam CT, Ng MN, Yu WC, Lau J, Wan T, Wang X, Yan Z, Liu H, Zhang Y, Fan ST. Gene expression profiling of liver cancer stem cells by RNA-sequencing. *PLoS ONE* 2012; 7 (5): e37159
11. Robinson MD, McCarthy DJ, Smyth GK. edgeR: a Bioconductor package for differential expression analysis of digital gene expression data. *Bioinformatics* 2010; 26(1): 139–140
12. Ho DW, Ng IO. uGPA: unified Gene Pathway Analyzer package for high-throughput genome-wide screening data provides mechanistic overview on human diseases. *Clin Chim Acta* 2015; 441: 105–108
13. Hong G, Zhang W, Li H, Shen X, Guo Z. Separate enrichment analysis of pathways for up- and downregulated genes. *J R Soc Interface* 2014; 11(92): 20130950
14. Aytes A, Mitrofanova A, Lefebvre C, Alvarez MJ, Castillo-Martin M, Zheng T, Eastham JA, Gopalan A, Pienta KJ, Shen MM, Califano A, Abate-Shen C. Cross-species regulatory network analysis identifies a synergistic interaction between FOXM1 and CENPF that drives prostate cancer malignancy. *Cancer Cell* 2014; 25(5): 638–651
15. Cummings RD, McEver RP. C-type lectins. In: Varki A, Cummings RD, Esko JD, Freeze HH, Stanley P, Bertozzi CR, Hart GW, Ertler ME. *Essentials of Glycobiology*. Cold Spring Harbor (NY): Cold Spring Harbor Laboratory Press, 2009
16. Uhlen M, Oksvold P, Fagerberg L, Lundberg E, Jonasson K, Forsberg M, Zwahlen M, Kampf C, Wester K, Hober S, Wernerus H, Björling L, Ponten F. Towards a knowledge-based Human Protein Atlas. *Nat Biotechnol* 2010; 28(12): 1248–1250
17. Bale TL, Giordano FJ, Hickey RP, Huang Y, Nath AK, Peterson KL, Vale WW, Lee KF. Corticotropin-releasing factor receptor 2 is a tonic suppressor of vascularization. *Proc Natl Acad Sci USA* 2002; 99(11): 7734–7739
18. Graziani G, Tentori L, Portarena I, Barbarino M, Tringali G, Pozzoli G, Navarra P. CRH inhibits cell growth of human endometrial adenocarcinoma cells via CRH-receptor 1-mediated activation of cAMP-PKA pathway. *Endocrinology* 2002; 143(3): 807–813
19. Hao Z, Huang Y, Cleman J, Jovin IS, Vale WW, Bale TL, Giordano FJ. Urocortin2 inhibits tumor growth via effects on vascularization and cell proliferation. *Proc Natl Acad Sci USA* 2008; 105(10): 3939–3944
20. Wang J, Xu Y, Xu Y, Zhu H, Zhang R, Zhang G, Li S. Urocortin's inhibition of tumor growth and angiogenesis in hepatocellular carcinoma via corticotrophin-releasing factor receptor 2. *Cancer Invest* 2008; 26(4): 359–368
21. Tezval H, Atschekzei F, Peters I, Waalkes S, Hennenlotter J, Stenzl A, Becker JU, Merseburger AS, Kuczyk MA, Serth J. Reduced mRNA expression level of corticotropin-releasing hormone-binding protein is associated with aggressive human kidney cancer. *BMC Cancer* 2013; 13(1): 199
22. Graña X, Reddy EP. Cell cycle control in mammalian cells: role of cyclins, cyclin dependent kinases (CDKs), growth suppressor genes and cyclin-dependent kinase inhibitors (CKIs). *Oncogene* 1995; 11 (2): 211–219
23. Lew DJ, Kornbluth S. Regulatory roles of cyclin dependent kinase phosphorylation in cell cycle control. *Curr Opin Cell Biol* 1996; 8 (6): 795–804
24. Nebert DW, Russell DW. Clinical importance of the cytochromes P450. *Lancet* 2002; 360(9340): 1155–1162
25. Denison MS, Whitlock JP Jr. Xenobiotic-inducible transcription of cytochrome P450 genes. *J Biol Chem* 1995; 270(31): 18175–18178
26. Guengerich FP. Common and uncommon cytochrome P450 reactions related to metabolism and chemical toxicity. *Chem Res Toxicol* 2001; 14(6): 611–650
27. Burkholder B, Huang RY, Burgess R, Luo S, Jones VS, Zhang W, Lv ZQ, Gao CY, Wang BL, Zhang YM, Huang RP. Tumor-induced perturbations of cytokines and immune cell networks. *Biochim Biophys Acta* 2014; 1845(2): 182–201
28. Lacy P, Stow JL. Cytokine release from innate immune cells: association with diverse membrane trafficking pathways. *Blood* 2011; 118(1): 9–18
29. Lippitz BE. Cytokine patterns in patients with cancer: a systematic review. *Lancet Oncol* 2013; 14(6): e218–e228